Effect of variation in the COPD breathing flow pattern on end-tidal CO2 tension: An *in vitro* study

Cletus F Adams, Mark C Jermy[1]*, Patrick H Geoghegan[2] and CJT Spence[3]

[1]Centre for Bioengineering, Department of Mechanical Engineering, University of Canterbury, New Zealand

[2]Biomedical Engineering, School of Life and Health Sciences, Aston University, Birmingham, UK

[3]Fisher & Paykel Healthcare, Auckland, New Zealand

Abstract

Aim: The goal of this work was to find out if the variation in breathing flow pattern alone (without change in tidal volume and respiratory rate) changes the end-tidal CO_2 tension ($EtCO_2$) enough to affect the health of a patient. The influence of I:E ratio on $EtCO_2$ was also investigated.

Method: Four breathing flow patterns belonging to different individuals diagnosed with COPD were collected from the literature. These were scaled to the same tidal volume, respiratory rate and I:E ratio, leaving shape as the only varying parameter. A programmable piston pump was used to reproduce the breathing flow patterns in an anatomically correct adult upper airway model (3D printed in acrylic, Visijet Ex200). CO_2 was simultaneously bled into the pump chamber at steady rate to mimic metabolic CO_2 production, followed by the measurement of $EtCO_2$ with and without 30 L/min of nasal high flow therapy.

Results: Breathing flow patterns varying in shape but not in tidal volume, respiratory rate and I:E ratio can produce statistically significant differences in $EtCO_2$. The variability in $EtCO_2$ was however found to be small (1 - 2%) and unlikely to be physiologically relevant. A 35% fall in I:E ratio corresponded to a 2% rise in $EtCO_2$. 30 L/min of NHF reduced $EtCO_2$ by approximately 20%.

Conclusion: Shape alone can cause a statistically significant difference in $EtCO_2$ however the difference in $EtCO_2$ is small. A 35% reduction in I:E ratio results in a 2% rise in $EtCO_2$.

Introduction

Arterial CO_2 tension modulates ventilation via a feedback mechanism. It is thus reasonable to hypothesise that each breathing pattern (though influenced by disease state) is optimized in terms of shape, amplitude and frequency to effect a specific change in CO_2 tension. Previous studies have explored how tidal volume, dead space volume, respiratory frequency and metabolic CO_2 rate influence $EtCO_2$. In a study by Parot, *et al.* [1] the respiratory frequency and metabolic CO_2 production in hypercapnic and non-hypercapnic COPD patients were found to be similar however the hypercapnic group showed a lower tidal volume. In hypercapnic individuals, the $EtCO_2$ correlates well with the ratio of dead space volume to tidal volume [2,3]. $EtCO_2$ has been reported to correlate well with arterial CO_2 Tension [4].

Critically ill patients suffering from COPD benefit from nasal high flow (NHF) therapy, which is the administration of warmed and humidified air at flow rates up to 8 L/min in neonates [5-7] and 60 L/min in adults [8]. NHF reduces the physiological dead space and respiratory frequency, and improves gas exchange [9-12].

The capnogram of a COPD patient is modulated by the degree of obstruction of the airways [13-15]. This obstruction, which affects the breathing flow pattern and magnitude, causes the capnogram of COPD patients to have a 'shark fin shape', [16] making them distinct from those of healthy individuals, which are more rectangular in shape [17]. Clinical studies on how a variation in the breathing flow pattern alone change $EtCO_2$ are scarce due to the difficulty in simultaneously maintaining the same tidal volume, peak airflow and I:E ratio over several breaths. In this report, an in-vitro study of the effect of breathing flow pattern, with and without NHF, on $EtCO_2$ is presented. Also the influence of I:E ratio variation on $EtCO_2$ is explored.

Methodology

Waveform collection

Four breathing flow patterns obtained from COPD patients (age range = 17 - 77 years, FEV1% pred = 36 - 63%) were collected from the literature. In three of these flow patterns [18-20], flow rate was plotted against time. In the remainder [21], the flow pattern was presented as a plot of tidal volume versus time which was numerically integrated to yield flow rate versus time plot after acquisition. Together with a healthy adult breathing flow waveform, which was previously used by Van Hove, *et al.* [22] and Spence, *et al.* [23] five waveforms were used in all.

A plot of all the waveforms collected is shown in Figure 1a. Note that positive flow represent inspiration and negative flow, expiration. The four COPD waveforms are designated as WF1, WF2, WF3 and WF4 with the healthy waveform labelled as WF5 (unmarked solid line). The COPD flow waveforms have a sharp concavity in the expiratory phase. It is noticeable that they vary in frequency and amplitude.

Normalization of waveforms

All the waveforms were normalized to the same tidal volume and respiratory rate via a linear rescaling of time axis followed by a

linear rescaling of the flow rate axis using different scaling factors for inspiratory and expiratory phases. Also, the inspired volume was matched to the expired volume. Two groups of breathing flow waveforms were obtained by scaling each breathing flow to two different I:E ratios i.e. 0.67 (IE1-group) and 0.43 (IE2-group), which corresponded to inspiratory time fractions of 40% and 30%. The fall in I:E ratio from 0.67 to 0.43 equals 35%. This change of 35% in I:E ratio was hypothesized to be sufficient to produce a significant change in $EtCO_2$. The breathing flow patterns

in the IE1-group and IE2-group are shown in Figures 1b and 1c respectively. Two different I:E ratios were needed to investigate the effect of I:E ratio on $EtCO_2$. The choice of I:E ratios were not without justification as Tobin, *et al.* [24] reported an I:E ratio of 0.73 ± 0.03 for healthy adults and 0.53 ± 0.05 for adult COPD patients.

Experimental setup

The experimental set-up is shown in Figure 2b. In the setup, a rigid upper airway model (3D-printed in acrylic, Visijet EX200) - Figure 2a - of an anonymous 44 year male adult (previously used by Spence, *et al.* [25] and Van Hove, *et al.* [22]) was connected to a piston pump. A CO_2 source was connected to the barrel of the piston pump via a rotameter. CO_2 was sampled at the trachea using a 20 Hz capnograph (MiniMediCO$_2$, manufactured by Oridion Medical Ltd., Israel). A mixing test conducted by placing a wire-gauze (to enhance mixing) at the entrance of the piston pump yielded no significant difference in $EtCO_2$ (< ± 3%). The volume of the piston chamber at the end of expiration (functional residual capacity) was maintained at 2500 ml for all experiments.

Experimental procedure

The pump forces the tracheal flow rate to follow the healthy waveform (WF5) in Figure 1b and Figure 1c. Metabolic CO_2 production was simulated by bleeding CO_2 at a flow rate of 98 scc/min (at a 20 KPa CO_2 source pressure) into the barrel of the piston pump. The end-tidal ($EtCO_2$) at this setting was 5.4% ± 0.3, which is comparable to the $EtCO_2$ of a resting healthy adult. CO_2 data was recorded before (zero-therapy, ZT) and during the application of 30 L/min of NHF (NHF30). An identical procedure was performed for all other waveforms with 6 repetitions for each.

Results

The capnogram was recorded for 20 consecutive breathing cycles for each experimental repeat. The 20 cycles of capnogram in repeat one (for healthy waveform (WF5) in IE1-group) have been superimposed and cascaded with those of the other repetitions as shown in Figure 3a. The variations in $EtCO_2$ from cycle to cycle is due to mixing. Figure 3b shows the average of all 120 capnograms (20 cycles in each of the 6 repeats) for WF5 (in IE1-group) with and without NHF. An identical plot is shown in Figure 3c for WF4 (a COPD waveform). Note the characteristic 'shark fin' shape of the COPD waveform (which is due to airway obstruction) [16].

The spontaneous breathing plots (for a no NHF condition) in Figure 3b and Figure 3c show a minimum CO_2 concentration of about 0.2% which is due to rebreathing of dead space CO_2 during inspiration. Note how this falls to 0.04% (atmospheric CO_2 concentration) when NHF of 30 L/min is applied. This indicates a reduction in re-inspired dead space CO_2 by NHF, which is in line with findings by Spence, *et al.* [23] and Van Hove, *et al.* [22] that NHF promotes mixing and flushes dead space CO_2. In Figure 3b and Figure 3c the $EtCO_2$ falls by approximately 20% when NHF of 30 L/min is applied.
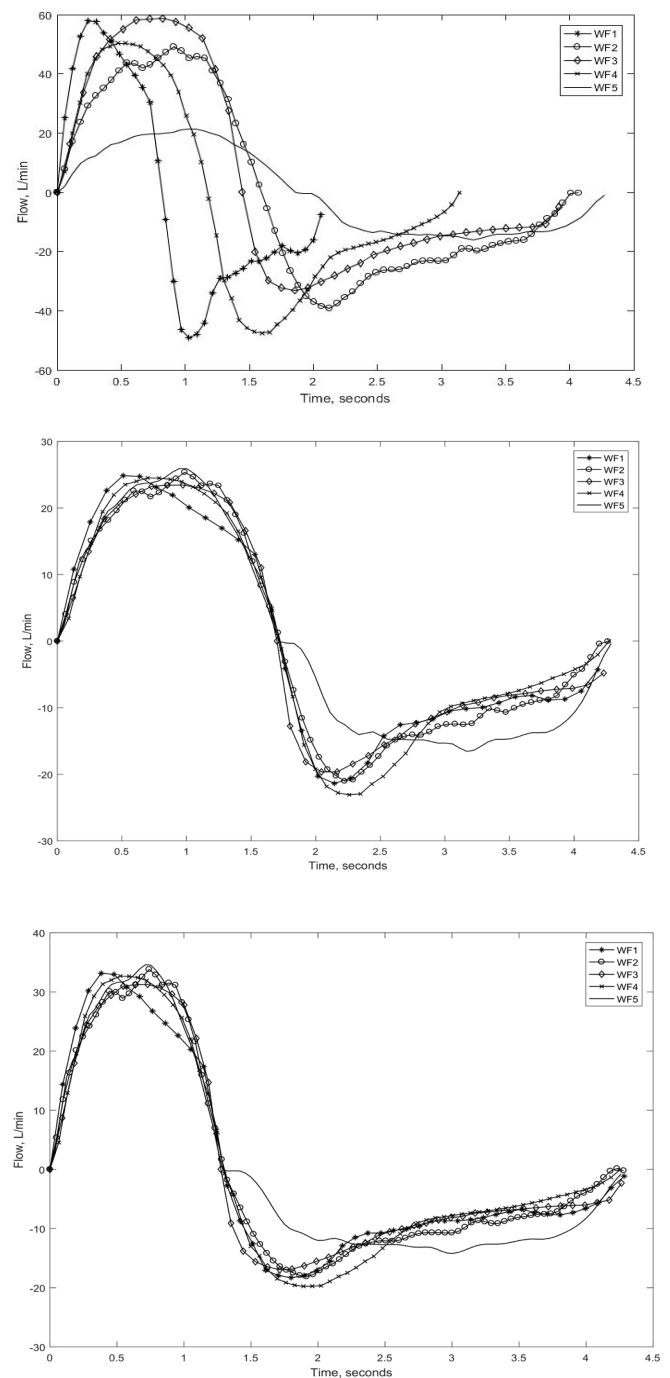

Figure 1. (a) All waveforms before scaling (b) IE1-group of flow waveforms (c) IE2-group of flow waveforms.

The average $EtCO_2$ (of 120 capnograms) for each waveforms (in both IE1-group and IE2-group) have been presented in Figure 4. The error bars represent two standard deviations in $EtCO_2$. In Figure 4, the $EtCO_2$ vary slightly between waveforms (e.g. see IE1-group waveforms) however the error bars overlap. Also pairs of plots belonging to the same waveform show some difference in $EtCO_2$ though error bars overlap (e.g. for label WF4 in Figure 4, compare the IE1-group and IE2-group pair).

The present finding shows that the characteristic shape of the COPD capnogram ('shark fin') - due to airway obstruction - can be
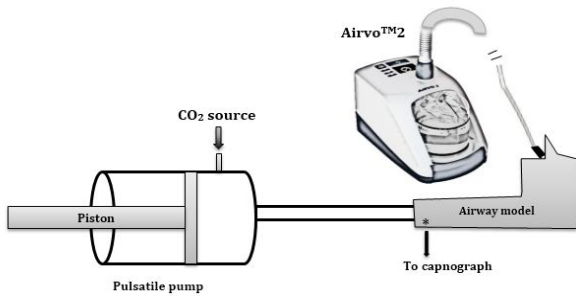
Figure 2. (a) Upper airway model (b) UAM is connected to the piston pump and AIRVO™2 device. CO_2 source is connected to piston pump for simulation of metabolic CO_2 production. CO_2 is sampled at the trachea during experiment.
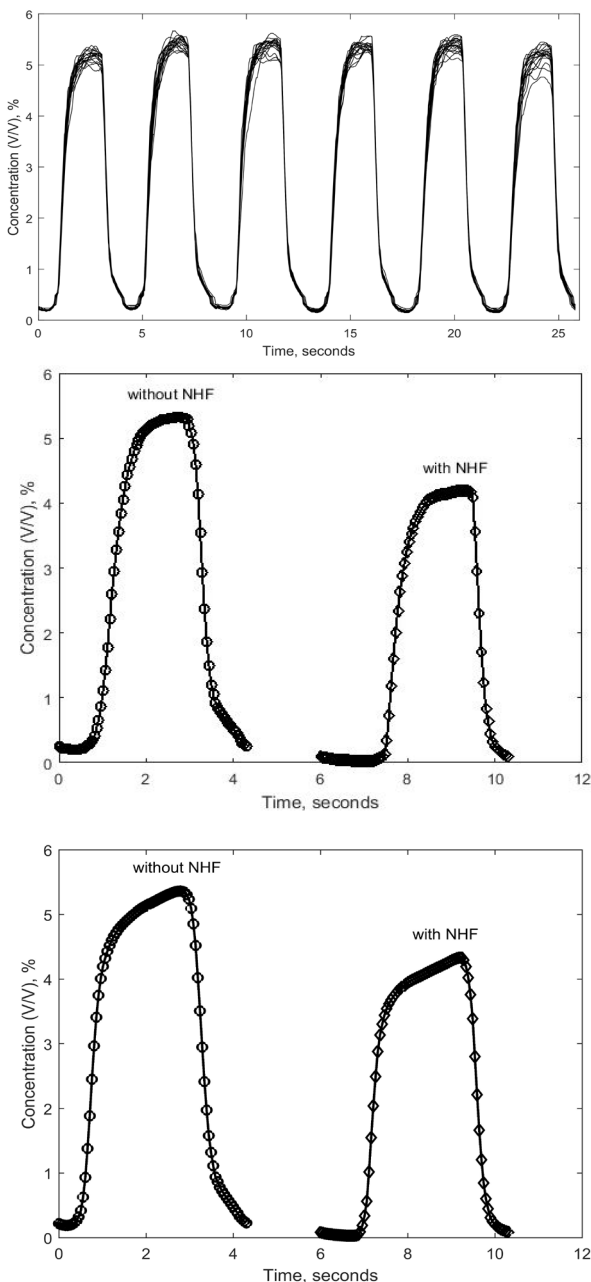
Figure 3. (a) A train of 6 capnograms for the healthy waveform (WF5) (b) Average of 120 capnograms for WF5 (c) Average of 120 capnograms for WF4.
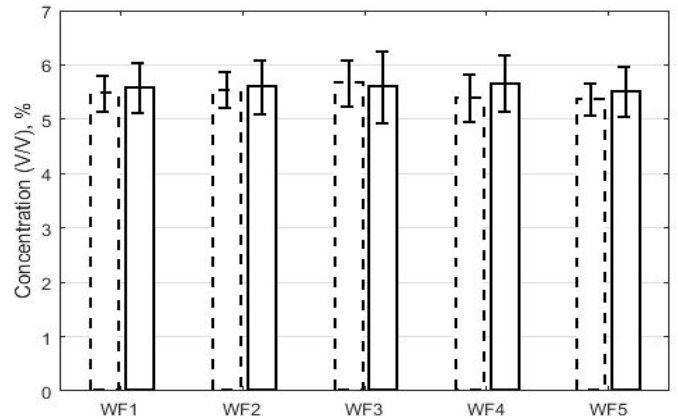
Figure 4. A plot of the average $EtCO_2$ of 120 capnograms associated with flow waveforms in both groups (IE1-group and IE2-group). The errorbars represent two standard deviations in $EtCO_2$ over the 120 capnograms.

reproduced from the corresponding breathing flow pattern. This supports the clinical reports that the breathing flow pattern modifies the shape of the capnogram [16]. Though error bar overlaps in $EtCO_2$ have been observed between and within the I:E ratio groups (IE-1 and IE-2) it is not conclusive if this means no statistically significant difference in $EtCO_2$ exists. In what follows a test of statistical difference in $EtCO_2$ is performed.

Test of statistical significance

A single factor ANOVA test was performed to find if the difference in $EtCO_2$ was statistically significant between different waveforms of the same I:E ratio. Further, a two sample t-test (assuming unequal variances) on pairs of $EtCO_2$ belonging to the same waveform but differing in I:E ratio was performed. In both tests, the critical value to confirm the null hypothesis was set to 0.02 instead of 0.05 to indicate a strong evidence against the null hypothesis. The results are presented in Table I, which shows evidence of statistically significant difference in $EtCO_2$ (p-value < 0.02) within the same group of I:E ratio (single factor ANOVA test, Table 1). Except for WF4, I:E ratio made a statistically significant difference in $EtCO_2$ (p-value < 0.02) in pairs belonging to the same I:E ratio (two-sample t-test, Table I). WF4 was not distinct in characteristics from the other waveforms.

Another two-sample t-test was performed for each I:E ratio group to find the specific pairings of flow waveforms that showed statistically significant difference in $EtCO_2$ as the single factor ANOVA test could not determine this. Note that 5 flow waveforms will yield 10 pairs. The results are presented in Table 2 in which 7 pairs (70%) - in bold ink – show statistically significant difference in $EtCO_2$ (p-value < 0.02) within the IE1-group. Only 4 pairs (40%) in the IE2 group have statistically significant differences in $EtCO_2$.

It is concluded that the differences in $EtCO_2$ of waveforms that are similar in all but pattern are statistically significant (p-value < 0.02) (a single factor ANOVA test, Table I). Also, $EtCO_2$ is sensitive to I:E ratio as 4 out of 5 flow waveforms (WF1, WF2, WF3 and WF5 but not WF4) showed a statistically significant difference in $EtCO_2$ (p-value < 0.02) (two sample t-test, Table 1). Furthermore, it is deduced from Table 2 that though statistically significant disparities in $EtCO_2$ was found in each group (Table 1), intragroup differences in $EtCO_2$ in the higher I:E ratio group (IE1-group, I:E ratio = 0.67) were more frequent (70%) than in the lower I:E ratio group (IE2-group, I:E ration = 0.47) - only 40% of the pairs showed a significant difference in $EtCO_2$.

Table 1. Results of a single factor ANOVA test and a two-sample t-test. A single factor ANOVA Test.

Groups (IE1 and IE2)	Sum of squares	df	Mean square	F	P-value
IE1	259	4	65	20	0.0001
IE2	84	4	21	5	0.0006
Two-sample t-Test					
	WF1	**WF2**	**WF3**	**WF4**	**WF5**
p-value	0.003	0.0001	0.002	0.05	0.002

Table 2. My caption.

p-value	WF1/WF2	WF1/WF3	WF1/WF4	WF1/WF5	WF2/WF3
IE1	0.068	0	0.048	0.017	0
IE2	0.03	0.105	0	0	0.32
p-value	**WF2/WF4**	**WF2/WF5**	**WF3/WF4**	**WF3/WF5**	**WF4/WF5**
IE1	0.08	0	0	0	0
IE2	0.036	0.031	0.015	0.013	0.49

Shape parameter and EtCO$_2$

Harmonic distortion (*Hd*) describes the degree to which a periodic signal deviates from a sinusoid [26]. It is mathematically expressed as:

$$Hd = \frac{\sqrt{H_2^2 + H_3^2 + H_4^2 + \ldots}}{H_1} \qquad (1)$$

where H_n is the root-mean-square amplitude of the nth harmonic (found using Fourier decomposition) of the waveform. n = 25 was used as beyond this, changes in *Hd* was found to be insignificant. *Hd* was computed for the entire breathing cycle, for the inspiratory phase and then the expiratory phase. EtCO$_2$ correlated better with a product of the inspiratory *Hd* and the peak inspiratory flow. This product is designated as *IDf*. The EtCO$_2$ and their corresponding *IDf* are presented in Figure 5. The Spearman's correlation coefficient (ρ) and error (2 standard deviations) in the measurement of EtCO$_2$ are also shown in Figure 5. The coefficient of determination (R2) (0.75 and 0.88) and ρ (0.9 and 1) indicate a strong correlation between IDf and EtCO$_2$ (Figure 5). It is not clear what implication this has for breathing.

In Equation 2, *average[EtCO2]$_{IE2}$* and *average[EtCO2]$_{IE1}$* are respectively, the average EtCO$_2$ in the IE1-group and IE2-group. Using the formula in Equation 2 the average EtCO$_2$ of the IE2-group was found to be 2% greater than that of the IE1-group. It is concluded that a 35% fall in I:E ratio (percentage difference between the I:E ratio of 0.67 (IE1-group) and 0.43 (IE2-group)) produces a 2% rise in EtCO$_2$.

$$\frac{average[EtCO_2]_{IE2} - average[EtCO_2]_{IE1}}{average[EtCO_2]_{IE1}} \qquad (2)$$

The coefficient of variability, defined as the ratio of the standard deviation in EtCO$_2$ within the group to the average EtCO$_2$ was found to be 2% and 1% respectively for the IE1-group and IE2-group.

Discussion

NHF reduces physiological dead space, respiratory frequency, and improves gas exchange [9-11]. The fall in EtCO$_2$ ($\approx$ 20%) upon the application of 30 L/min of NHF supports the report that NHF improves mixing and reduces the proportion of CO$_2$ in re-inspired dead space air [9,22,23]. The present data suggests that breathing flow waveforms of different patterns, but similar in tidal volume, period and I:E ratio show statistically significant differences in EtCO$_2$. Further, the results indicate that two breathing waveforms that differ only in I:E ratio can

produce different EtCO$_2$. If that tidal volume and respiratory rate are fixed, it is more probable to find a statistically significant difference in EtCO$_2$ between a greater I:E ratio group than those of a lower I:E ratio.

To preserve tidal volume, a fall in I:E ratio (longer expiration, shorter inspiration) is matched by a rise in peak inspiratory breathing flow and a fall in peak expiratory breathing flow. In Figure 4, the EtCO$_2$ corresponding to the lower I:E ratio i.e. 0.46 (IE2-group) tended to be greater. Tobin, *et al.* [24] observed that the inspiratory time (Ti) of 28 COPD subjects (mean age = 67.5 years) was 1 second less than that of healthy adults. Sorli, *et al.* [27] concluded that CO$_2$ retention (marked by higher EtCO$_2$) in COPD patients is due to shallow breathing, which arises from reduced Ti. This suggests the higher EtCO$_2$ is due to less efficient purging of the dead space during inspiration, i.e. lower ratio of inspired volume to dead space volume resulting in less complete replacement of dead space gas with fresh air (residual volume of expired gas mixes with a smaller volume of fresh gas). This is in unison with the observation by Gorini, *et al.* [28] who found the highest arterial partial pressure of CO$_2$ amongst COPD patients with the smallest Ti. IE1-group and IE2-group differed in Ti by 0.43 seconds. In the present data, a fall in I:E ratio by 35% (0.67 to 0.43) corresponded to 2% rise in EtCO$_2$. Though the present results agrees qualitatively with findings in the literature [24,27,28] it is concluded that the fall in EtCO$_2$ due to a fall in I:E ratio by 35% is small (2%). The variability in EtCO$_2$ due to flow pattern difference is 1 - 2%. Though statistically significant, it is also small.

The product of inspiratory flow and inspiratory harmonic distortion (*IDf*) correlate well with EtCO$_2$. The expiratory breathing flow has been reported to be modulated by the inspiratory flow pattern [26]. Inspiratory muscle dysfunction increases EtCO$_2$. Begin, *et al.* [29] found that airway resistance correlated well with arterial CO$_2$ tension, which also correlates well with EtCO$_2$ [30]. In a study by Loveridge, *et al.* [31] healthy subjects were observed to show a greater variability in breathing pattern than COPD subjects. Since airway obstruction during COPD influences EtCO$_2$ and the flow pattern, it is speculated that *IDf* is related to the ventilatory response to CO$_2$ tension.

Limitations of this work

The piston chamber is rigid, unlike the human lung which is compliant (lung compliance is $\approx$ 200 mL/cmH$_2$O for healthy young adults). Note that a constant bleed rate differs from the physiologically realistic system in which CO$_2$ flow is distributed over time. Also, this work is limited by the number of breathing flow patterns used.
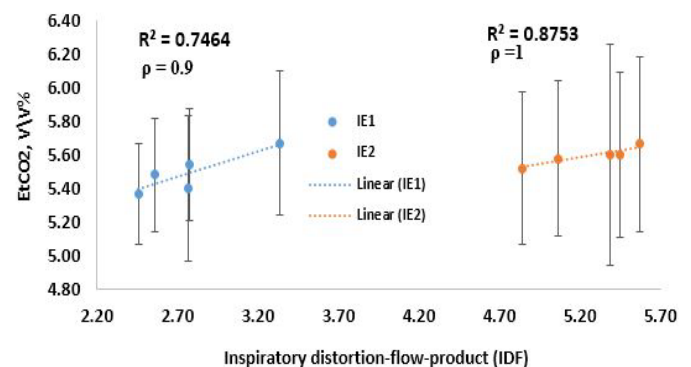
Figure 5. plot of EtCO2 against IDf.

Conclusion

Breathing patterns similar in tidal volume, respiratory rate, and I:E ratio but differing in shape can produce statistically significant difference in $EtCO_2$ however the variability is small (1 - 2%). A 35% fall in I:E ratio of breathing waveforms with no change in tidal volume and respiratory rate produces only a 2% rise in $EtCO_2$. NHF of 30 L/min reduces $EtCO_2$ by 20%.

Acknowledgment

References

1. Parot S, Saunier C, Gautier H, Milic-Emili J, Sadoul P (1980) Breathing pattern and hypercapnia in patients with obstructive pulmonary disease. *American Review of Respiratory Disease* 121: 985-991.

2. Calverley PMA (2003) Respiratory failure in chronic obstructive pulmonary disease. *European Respiratory Journal* 22: 26s-30s.

3. Blanch L, Romero PV, Lucangelo U (2006) Volumetric capnography in the mechanically ventilated patient. *Minerva Anestesiol* 72: 577-586. [Crossref]

4. Nagler J, Krauss B (2009) Capnographic monitoring in respiratory emergencies. *Clinical Pediatric Emergency Medicine* 10: 82-89.

5. Manley BJ, Owen LS, Doyle LW, Andersen CC, Cartwright DW, et al. (2013) High-flow nasal cannulae in very preterm infants after extubation. *N Engl J Med* 369: 1425-1433. [Crossref]

6. Motojima Y, Ito M, Oka S, Uchiyama A, Tamura M, et al. (2016) Use of high-flow nasal cannula in neonates: Nationwide survey in Japan. *Pediatr Int* 58: 308-310. [Crossref]

7. Ojha S, Gridley E, Dorling J (2013) Use of heated humidified high-flow nasal cannula oxygen in neonates: a UK wide survey. *Acta Paediatr* 102: 249-253. [Crossref]

8. Ward JJ (2013) High-flow oxygen administration by nasal cannula for adult and perinatal patients. *Respir Care* 58: 98-122. [Crossref]

9. Dysart K, Miller TL, Wolfson MR, Shaffer TH (2009) Research in high flow therapy: mechanisms of action. *Respir Med* 103: 1400-1405. [Crossref]

10. Riera J, Pérez P, Cortés J, Roca O, Masclans JR, et al. (2013) Effect of high-flow nasal cannula and body position on end-expiratory lung volume: a cohort study using electrical impedance tomography. *Respir Care* 58: 589-596. [Crossref]

11. Mündel T, Feng S, Tatkov S, Schneider H (2013) Mechanisms of nasal high flow on ventilation during wakefulness and sleep. *J Appl Physiol (1985)* 114: 1058-1065. [Crossref]

12. Sztrymf B, Messika J, Bertrand F, Hurel D, Leon R, et al. (2011) Beneficial effects of humidified high flow nasal oxygen in critical care patients: a prospective pilot study. *Intensive Care Med* 37: 1780-1786. [Crossref]

13. You B, Peslin R, Duvivier C, Vu VD, Grilliat JP (1994) Expiratory capnography in asthma: evaluation of various shape indices. *Eur Respir J* 7: 318-323. [Crossref]

14. Krauss B, Hess DR (2007) Capnography for procedural sedation and analgesia in the emergency department. *Ann Emerg Med* 50: 172-181. [Crossref]

15. Gluncic TJ, Basara L, Konecki L, Tomic S, Samarzija M, et al. (2015) Capnographic measurement as a screening method for respiratory obstructive diseases. *European Respiratory Journal* 46: 1039.

16. Mieloszyk RJ, Verghese GC, Deitch K, Cooney B, Khalid A, et al. (2014) Automated quantitative analysis of capnogram shape for COPD-normal and COPD-CHF classification. *IEEE Trans Biomed Eng* 61: 2882-2890. [Crossref]

17. Jaffe MB (2006) Volumetric capnography, the next advance in CO_2 monitoring. Respironics Inc (Critical Care).

18. Colasanti RL, Morris MJ, Madgwick RG, Sutton L, Williams EM (2004) Analysis of tidal breathing profiles in cystic fibrosis and COPD. *Chest* 125: 901-908. [Crossref]

19. Williams EM, Powell T, Eriksen M, Neill P, Colasanti R (2014) A pilot study quantifying the shape of tidal breathing waveforms using centroids in health and COPD. *J Clin Monit Comput* 28: 67-74. [Crossref]

20. Dellacà RL, Santus P, Aliverti A, Stevenson N, Centanni S, et al. (2004) Detection of expiratory flow limitation in COPD using the forced oscillation technique. *European Respiratory Journal* 23: 232-240.

21. Dellacà RL, Pompilio PP, Walker PP, Duffy N, Pedotti A, et al. (2009) Effect of bronchodilation on expiratory flow limitation and resting lung mechanics in COPD. *Eur Respir J* 33: 1329-1337. [Crossref]

22. Van Hove SC, Storey J, Adams C, Dey K, Geoghegan PH, et al. (2016) An experimental and numerical investigation of CO2 distribution in the upper airways during nasal high flow therapy. *Ann Biomed Eng* 44: 3007-3019. [Crossref]

23. Spence CJT, Buchmann NA, Jermy MC (2012) Unsteady flow in the nasal cavity with high flow therapy measured by stereoscopic PIV. *Experiments in Fluids* 52: 569-579.

24. Tobin MJ, Chadha TS, Jenouri G, Birch SJ, Gazeroglu HB, Sackner MA (1983) Breathing patterns. 2. diseased subjects. *Chest* 84: 286-294. [Crossref]

25. Spence CJT, Buchmann NA, Jermy MC, Moore SM (2011) Stereoscopic PIV measurements of flow in the nasal cavity with high flow therapy. *Experiments in Fluids* 50: 1005-1017.

26. Frey U, Silverman M, Suki B (2001) Analysis of the harmonic content of the tidal flow waveforms in infants. *J Appl Physiol (1985)* 91: 1687-1693. [Crossref]

27. Sorli J, Grassino A, Lorange G, Milic-Emili J (1978) Control of breathing in patients with chronic obstructive lung disease. *Clin Sci Mol Med* 54: 295-304. [Crossref]

28. Gorini M, Misuri G, Corrado A, Duranti R, Iandelli I, et al. (1996) Breathing pattern and carbon dioxide retention in severe chronic obstructive pulmonary disease. *Thorax* 51: 677-683. [Crossref]

29. Begin P, Grassino A (1991) Inspiratory muscle dysfunction and chronic hypercapnia in chronic obstructive pulmonary disease. *Am Rev Respir Dis* 143: 905-912. [Crossref]

30. McSwain SD, Hamel DS, Smith PB, Gentile MA, Srinivasan S, et al. (2010) End-tidal and arterial carbon dioxide measurements correlate across all levels of physiologic dead space. *Respir Care* 55: 288-293. [Crossref]

31. Loveridge B, West P, Anthonisen NR, Kryger MH (1984) Breathing patterns in patients with chronic obstructive pulmonary disease. *Am Rev Respir Dis* 130: 730-733. [Crossref]